Investigation of Longitudinal Dynamics of Vehicles in Disordered Traffic

Madhuri Kashyap N R

Department of Civil and Environmental Engineering Indian Institute of Technology Tirupati Email: ce19d003@iittp.ac.in

Gowri Asaithambi*

Department of Civil and Environmental Engineering Indian Institute of Technology Tirupati Email: gowri@iittp.ac.in

Martin Treiber

Institute for Transport & Economics
Technical University Dresden Germany
Email: mail@martin-treiber.de

and

Venkatesan Kanagaraj

Department of Civil Engineering Indian Institute of Technology Kanpur Email: venkatk@iitk.ac.in

* Corresponding Author

Abstract

Vehicles in developing countries have wide variations in their static and dynamic characteristics, and drivers tend to not follow lane discipline. Models for driving behavior under such disordered traffic conditions need to include the vehicle dynamics and their interactions with the surrounding environment. Calibration of those models is necessary to evaluate their predictive power and suitability for analyzing traffic flow under disordered traffic. The present study aims to calibrate a longitudinal dynamics model, the High-Speed Social-Force Model (HSFM) using a vehicle trajectory dataset collected from Chennai city. The HSFM was calibrated by minimizing the deviations between the simulated and observed longitudinal coordinates of vehicles using a genetic algorithm. The observed and simulated vehicle trajectories were compared using a goodness of fit function of the positions. The convergence of the objective function has been illustrated with the help of fitness landscapes. The calibration errors were found to be within the acceptable range and the optimal parameter values were found to be consistent. The outcomes of the study indicate that the model can capture the influence of non-overlapping leaders under disordered traffic conditions.

Keywords: Longitudinal Dynamics, High-Speed Social-Force Model, Calibration, Vehicle Trajectory Data, Disordered Traffic

1. Introduction and Background

Modeling traffic flow is generally carried out in two ways, modeling the aggregate characteristics of a traffic stream (macroscopic) and modeling the individual vehicle dynamics (microscopic). Microscopic traffic flow models constitute the most suitable model class to simulate and understand the dynamics of heterogeneous vehicles and the interactions of their drivers with other vehicles and the environment, particularly for disordered traffic flow. Traditionally, microscopic models are classified into two categories: car-following and lane-changing models. The car-following models are used to model the vehicular movements in the longitudinal direction whereas lane-changing models replicate the lateral movements [1]. The car-following models are categorized as stimulus-response or GHR (Ghazis-Herman-Rothary) models, psychophysical models, collision-avoidance models, safety distance models, fuzzy logic-based models, optimal velocity models, and other variants [1]. The basic assumption of these models is that the vehicle moves in the middle of the lane and therefore, the leader and follower are present in the same lane [2].

In the case of ordered traffic, the distribution of vehicles' lateral positions inside the lane follows essentially a normal distribution and there is no need to include the lateral displacement between leader and follower to the model input. However, this normality is lost in disordered traffic [3]. Disordered traffic refers to the wide mix of different vehicle types such as cars, two-wheelers, trucks, buses, auto-rickshaws, etc. utilizing the complete roadway without lane discipline, as observed in South-Asian countries like India. Under such conditions, the longitudinal acceleration of the follower depends not only on the longitudinal gap to the immediate leader and the speeds but also on the lateral displacement (staggered leaders) and possibly on several leaders. There are even situations where it is difficult to identify the most relevant leader since, due to the very dynamic nature of such traffic flow with many overtaking and passing maneuvers, not only the lateral displacement and the longitudinal gap but also the relative speed determines the leader having the highest influence on the follower [4,5].

A car-following model is said to be complete if it can capture the appropriate longitudinal acceleration in all possible traffic situations including free acceleration, free cruising, approaching, steady-state and dynamic following, stopped traffic, and highly dynamic emergency situations [6]. Simple complete models include the Optimal Velocity Model, the Gipps model, and the Intelligent Driver Model (IDM). From these models, only the IDM satisfies further requirements such as having realistic accelerations and being accident-free [6]. However, it is only applicable to ordered lane-based traffic flow.

The calibration of microscopic traffic flow models is a significant step that needs to be carried out to predict vehicular movements and evaluate the applicability of these models in the traffic stream. While there are many works on calibrating lane-based car-following models (see, e.g., [7] or [8]), few researchers attempted to formulate models for disordered traffic conditions and calibrate their longitudinal dynamics. In these attempts, the lane-based car-following models are usually augmented by a simple factor based on the lateral displacement and restricted to proper car-following, i.e., no situations where the nearest vehicles are on the side (no-following mode). This includes calibrating the modified General Motors model [9], the Gipps model [10,11], the Wiedemann model [12,13], the Optimal velocity model [14,15], and the Intelligent driver model [16,17]. None of the above investigations included non-following modes where there could be different leaders influencing the subject vehicle at different time instances. Moreover, the above

calibrations were based on real-world trajectory data for very short sections (250 m at most) and carried out using macroscopic variables as the measure of performance only probing for the aggregated behavior rather than the individual driving behavior.

To our knowledge, there are only two attempts made to model including all situations that may arise in disordered traffic including no-following situations, namely the High-Speed Social Force Model (HSFM[18]) and the Intelligent Agent Model (IAM [19]) which improved the HSFM by simplifying it and also generalizing it by considering social forces from all vehicles in the neighborhood, including the followers. When only considering the longitudinal dynamics and ignoring the social forces of the followers, the HSFM is equivalent to the IAM.

In this study, we microscopically calibrate the HSFM specialized to the IDM for longitudinal dynamics using trajectory data collected at an urban arterial in Chennai city under disordered traffic conditions. We verified that the calibrated parameter values correspond to the respective global minimum of the vehicle's position-related objective function. While the calibrated parameters of the car-following component were consistent with past investigations, we also estimate, to our knowledge for the first time, model parameters related to lateral offsets of the leader.

The major contributions of this study are the following: 1) Calibrating, for the first time, all the cases of longitudinal movement such as laterally overlapping (car-following behavior) and non-overlapping cases, 2) including changing leaders and dynamically identifying the most interacting vehicle, 3) calibrating to a microscopic measure of performance using a novel protocol giving insight into individual driver responses to a laterally changing environment, 4) using significantly longer trajectory data collected under disordered traffic conditions than that used in the previous studies.

The formulations involved in the HSFM are discussed in the next section. The third section describes the data used in the study and the calibration methodology, and the fourth section discusses the results followed by the conclusion.

2. High-Speed Social-Force Model

The High-Speed Social-Force Model (HSFM) is developed based on the concept of social forces to model the directed flow of high-speed self-driven particles such as vehicles in traffic stream [18]. Figure 1 presents the formulation of the HSFM which predicts the longitudinal acceleration of the vehicle for the future time step. The model consists of three components: self-driven acceleration, interaction force, and external forces given by the following equation:

$$\frac{dv_i}{dt} = f_i^{self} + f_{il'} + \sum_b f_{ib} \tag{1}$$

Where,

 $\frac{dv_i}{dt} = Acceleration of vehicle i$

 $f_i^{\tilde{self}} = Self driven acceleration$

 $f_{il^{\prime}} = Interaction \ acceleration \ with \ the \ most \ interacting \ vehicle$

 $f_{ib} = Acceleration due to external forces such as road boundaries (b)$

l' = Most interacting leader

In Equation 1, the f_i^{self} and $f_{il'}$ are computed using Intelligent Driver Model given by the following equation:

$$a^{CF}(s_{il}, v_i, v_l) = a^{CF, free}(v_i) + a^{CF, int}(s_{il}, v_i, v_l)$$

$$= a \left[1 - \left(\frac{v_i}{v_0} \right)^{\delta} - \left(\frac{s^*(v_i, v_l)}{s_{il}} \right)^2 \right]$$
(2)

Where,

 $a = Maximum \ acceleration$

 $v_0 = Desired speed$

 $v_i = Longitudinal speed of vehicle i$

 $v_l = Longitudinal speed of leader l$

$$s^*(v_i, v_l) = Desired\ distance = s_0 + max\left(0, v_i T + \frac{v_i(v_i - v_l)}{2\sqrt{ab}}\right)$$

 s_{il} = Longitudinal gap between vehicle i and leader $l = x_l - x_i - lveh_l$

 $lveh_l = Length \ of \ leader \ vehicle$

 $s_0 = Minimum spacing$

T = Desired time gap

b = Comfortable deceleration

The first part of the Equation (2) is the acceleration of vehicle when it is free to move without any interaction with the surroundings. It is calculated using the Intelligent Driver Model under free acceleration condition as given below:

$$f_i^{self} = a^{CF,free}(v_i) = a^{CF}(\infty, v_i, v_l)$$
(3)

The interaction of the vehicle with the leaders is considered in the second part of the Equation (2). The identification of the leaders is a significant part of the HSFM. Initially, the threshold up to which other vehicles may have an influence on the vehicle (Influencing Length) is computed based on maximum desired speed and desired time gap as shown in equation 4. Any vehicle over the entire road width that is longitudinally ahead of the subject vehicle within the influencing length is identified as a potential leader (Figure 2).

Influencing Length =
$$L + (v_0 T + 0.5 \frac{v_0^2}{b})$$
 (4)

Where L=vehicle length in m; v_0 = maximum desired speed (considered as 25 m/s); T= desired time gap (taken as 1 s); b = deceleration (considered as 4 m/s²)

Then, the interaction force (acceleration) f_{il} of each potential leader is computed for all potential leaders l and the vehicle l' causing the most negative force (largest deceleration) is selected as the only leader. The interaction force is equal to the IDM interaction acceleration valid for strict carfollowing multiplied with the lateral attenuation factor $\alpha(\Delta y_{il})$ reflecting a decreasing effect for lateral displacements of the leader,

$$f_{il}(\Delta x_{il}, \Delta y_{il}, v_i, v_l) = \alpha^{CF, int}(\Delta x_{il}, v_i, v_l)\alpha(\Delta y_{il})$$
(5)

with

$$a^{CF,int}(\Delta x_{il}, v_i, v_l) = a^{CF}(\Delta x_{il} - lveh_l, v_i, v_l) - a^{CF,free}(v_i)$$
(6)

and

$$\alpha(\Delta y_{il}) = \min\left\{\exp\left(-\frac{s_{il}^{y}}{s_{0}^{y}}\right), 1\right\}$$
 (7)

The lateral attenuation factor α with the lateral attenuation scale s_0^y as a model parameter is formulated based on the assumption that the influence of leader varies exponentially with a positive lateral gap $s_{il}^y = |\Delta y_{il}| - (w_i + w_l)/2$ between leader l and the subject vehicle i (w_i and w_l are the vehicle widths, see Fig. 2) while $\alpha = 1$ if the leader is longitudinally overlapping with the subject vehicle $s_{il}^y < 0$ since, then, a negative longitudinal gap ($gap = X_{leader} - X_{follower} - L_{Leader}$) will mean a crash.

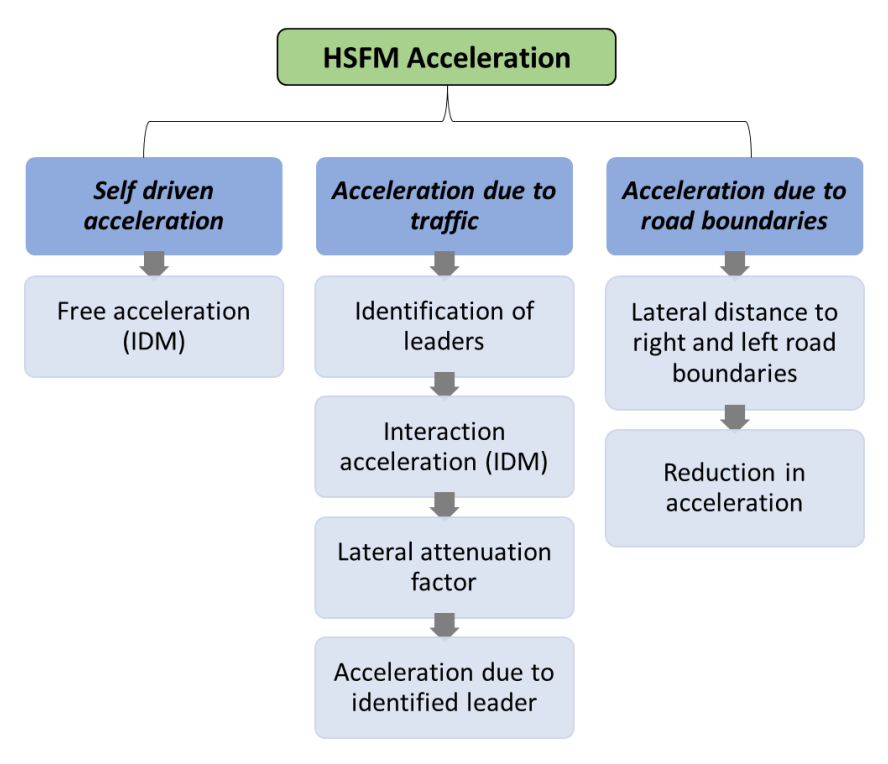


Figure 1 Formulation of HSFM

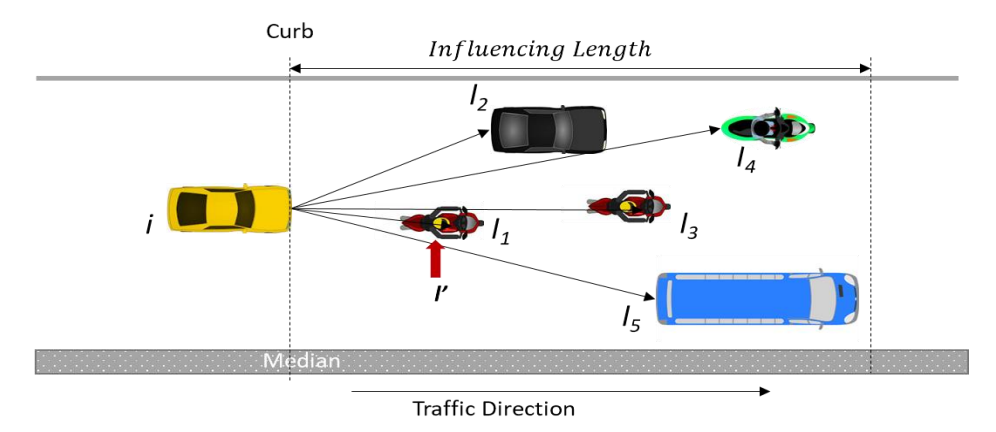


Figure 2 Identification of potential leaders (*Note: i - Subject vehicle, l – Leader, l' - Most influencing leader*)

The last part of the social force model consists of the influence due to external forces such as traffic signals, road boundaries and other obstacles [18]. Since, this study deals with modeling vehicular movements away from intersections, the influence of road boundaries has been taken into consideration, only. Similarly, to the lateral attenuation of the force from other vehicles, the boundary effect decreases exponentially with the lateral distance $b \pm y$ to the boundaries where b is the half-width of the road, and y is the lateral distance from the road center. For both left and right boundaries together, we thus obtain

$$\sum_{b} f_{ib} = f_{b} \left[-e^{\left(-\left(\frac{b+y}{s_{0b}^{y}} \right) \right)} - e^{\left(-\left(\frac{b-y}{s_{0b}^{y}} \right) \right)} \right]$$
 (8)

Where, $-f_b$ denotes the repulsive force if the vehicle center is immediately at one of the boundaries and s_{0b}^{y} denotes the road boundary scale. Notice that, unlike the expression for the vehicle-vehicle interaction, there is no cutoff for negative lateral gaps $b - |y| - w_i/2$ reflecting the fact that the situation gets worse with the degree the vehicle leaves the road.

3. Calibration Framework

Calibration refers to the determination of the model parameters such that the simulation is closest to the observations according to a goodness-of-fit function (GoF) based on a measure of performance (MoP) [20]. There are two approaches generally followed for calibration of microscopic models namely, local and global. The local approach makes predictions for only one future time step. For acceleration-based models, this means comparing the observed acceleration with the acceleration as modeled for the actual observed speeds and positions, step by step. The global approach predicts the entire vehicle trajectory based on initial state variables. Since the system dynamics correlates future position and speed values with the present acceleration returned by the model, the global approach includes more aspects of traffic flow and is more robust to measurement errors [6] and therefore has been adopted in the current study. The data used for calibration and the simulation set-up is discussed in the following subsection.

3.1 Data

We use vehicle trajectory data collected on a six-lane divided urban arterial road in Chennai city under disordered traffic conditions (wide mix of vehicles and lane-free traffic; the drivers generally did not obey the visible lane markings). Videos were obtained from four UAVs (unmanned aerial vehicles), simultaneously deployed to cover a length of 605 m over the road stretch. The vehicles were tracked in every frame of the videos using a semi-automated tool, and the trajectories from the four UAVs were stitched together. The average flow in the study section is 6720 veh/h which corresponds to moderate traffic conditions. The traffic stream comprises 50% two-wheelers, 40% cars, and 10% other categories (auto-rickshaws, buses, trucks, and light commercial vehicles). In total, 856 trajectories were extracted at a 0.5 sec time interval. Even for such a comparatively large sample time interval, large acceleration noise is produced by the double-time differentiation of the primary position data. To remove most of the noise and remain kinematically consistent, the positional data were smoothed by a symmetric exponential moving average filter (sEMA) of kernel width 0.5 s. Speeds and accelerations were obtained by numerical differentiation using the central difference method without further smoothing. Further details of the data are available in [15].

This study is mainly focused on the longitudinal dynamics of vehicles and therefore, it was ensured that only vehicle trajectories without significant lateral movements were considered. Specifically, the trajectories were filtered for a maximum lateral deviation of 0.5 m from the initial lateral position and for a minimum time duration of 30 s [21]. Figure 3 shows an example of such a trajectory. In total, 102 samples have been obtained among which cars and two-wheelers are dominant. It can be seen from Figure 3b that the trajectory data is essentially free from lateral movements. Notice that each of these trajectories may have more than one leader during the sampled time interval.

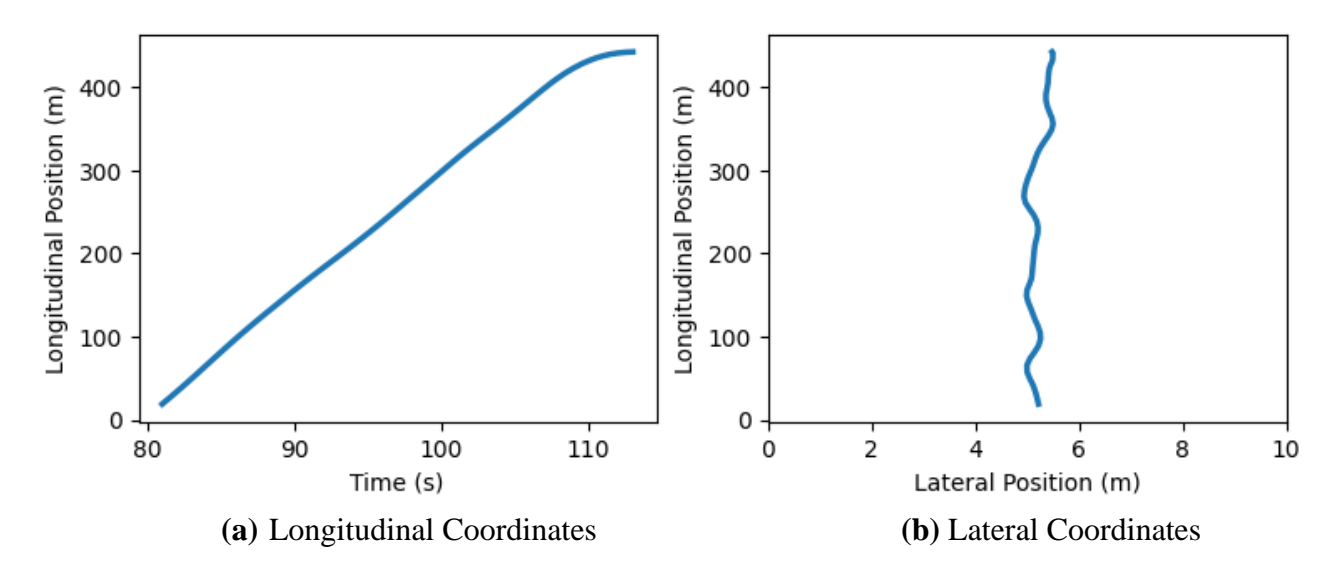


Figure 3 Visualization of a filtered sample trajectory

3.2 Simulation Set-up

The simulation of a trajectory here refers to predicting the longitudinal acceleration, speed, and position for all time instants t = idt, dt = 0.5 s, where data points exist. At t = 0, the simulated

vehicle is initialized to the position (x(0), y(0)) and the longitudinal speed v(0) given by the data. For each time step t=idt, the complete environment, i.e., all other trajectories as well as the lateral position of the considered trajectory is updated by the data (Figure 4) while the longitudinal acceleration a(t)=dv(t)/dt is simulated using the High-speed Social Force model (HSFM). To prepare for the next time step t+dt, the speed and longitudinal position is calculated using the ballistic update rules v(t+dt)=v(t)+a(t)dt, $x(t+dt)=x(t)+v(t)dt+0.5a(t)dt^2$, respectively, $a(t)=dv_i/dt$ is given by Equation (1).

The calibration process is defined by the Measure of Performance (MoP), the objective function or goodness-of-fit function (GoF), and the optimization algorithm. Possible microscopic MoPs include position, speed, acceleration, relative speed (speed difference), and the space gap. In this study, we will use the longitudinal position of the vehicle for the following reasons. (i) In contrast to the relative speed or the space gap, it is not sensitive to changes of the leader vehicle, so it is differentiable and easier to calibrate. Moreover, it does not use non-measurable internal model variables (which leader to use, i.e., which gap to take is a model property). (ii) In contrast to the speed and acceleration, the position is directly observable and takes care of the serial correlations implicit in the dynamics, and it is therefore to be preferred [22]. Regarding the GoF, using the position instead of the gap as MoP comes at the price of needing to use absolute errors because relative errors are not sensibly defined for positions. Specifically, we use the Root Mean Square Error (RMSE) as the GoF in this study (Equation 8).

$$E = \sqrt{\sum_{i=1}^{n} (x_i - x_i^{obs})^2 / n}$$
 (9)

Where,

E = Root Mean Square Error

 $x_i, x_i^{obs} = Simulated and Observed position of vehicle at ith data point respectively <math>n = Total$ number of data points in trajectory of the vehicle

Figure 4 visualizes the calibration process. At t=326 s the subject vehicle is initialized with the data. At each simulation step, the most influential leader is identified, and the subject's longitudinal position is determined by the HSFM with the ballistic update while the lateral position is set by the data. Between t=327.5 and 328 s, the most influential leader changes and the positive positional error increasing before the leader change is reduced, presumably by the stronger repulsive effect of the new leader. The space gap vs time plots illustrate the cases of vehicles having more than one leader (Figure 9). It can be observed that there is discontinuity in space gap curve due to a change of the most influencing leader. This shows us that the longitudinal position of the vehicle is a better MoP than the longitudinal gap. Moreover, since the longitudinal gap depends on the most influential leader, i.e., on the model, it cannot be observed in the data.

In order to find the solution for the non-linear optimization problem of minimizing the RMSE (Equation 8) with respect to the parameters thereby performing the calibration, genetic algorithm (GA) is applied [6]. Several researchers have adapted GA for calibrating driving behavior models

in the past [14,15,23-25]. For each sample trajectory, an individual set of optimal/calibrated parameters was determined thus considering inter-driver variations. The boundaries of allowed HSFM parameters ranges (Table 1) were defined based on the literature [18,21].

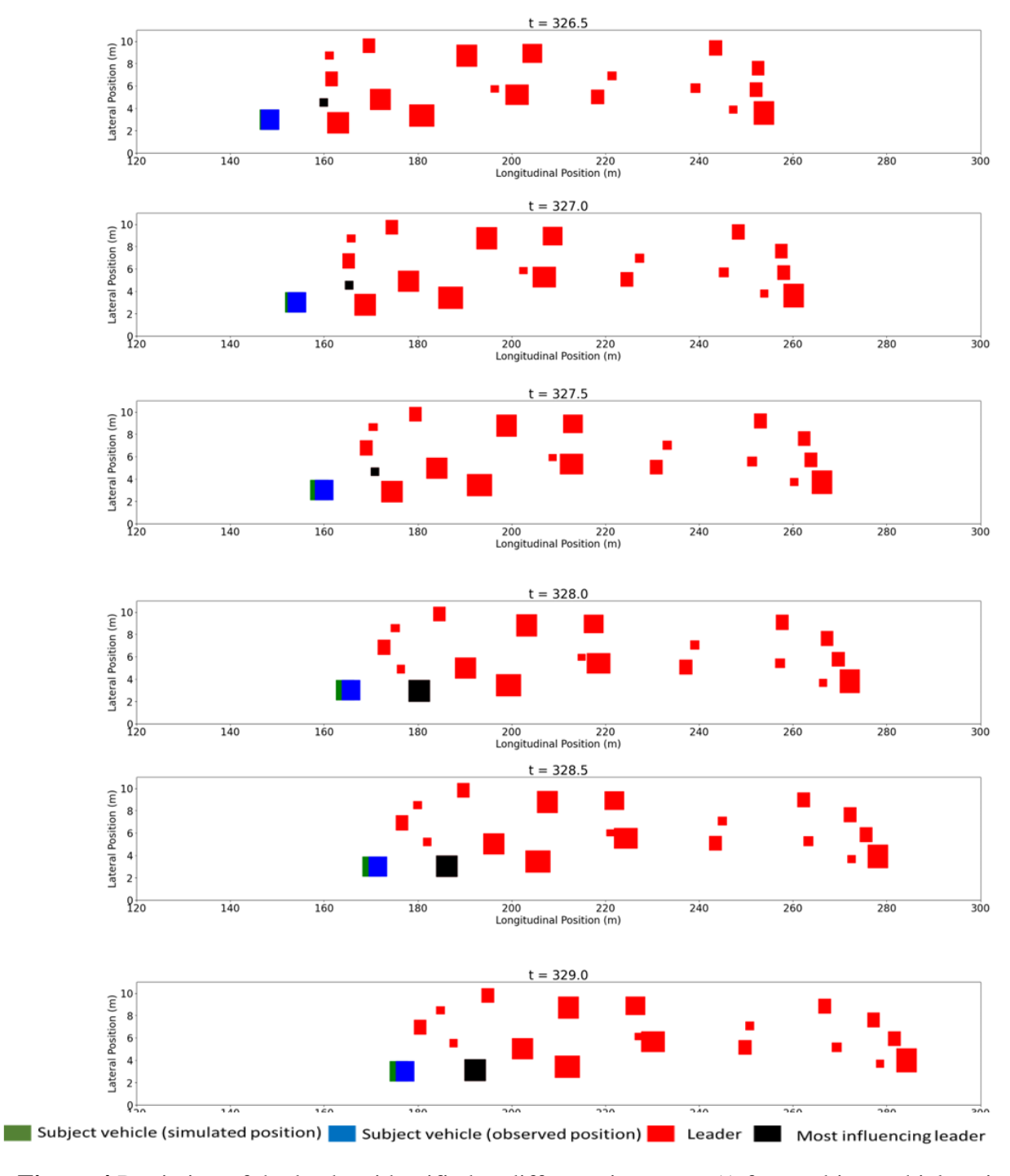


Figure 4 Depiction of the leaders identified at different time steps (t) for a subject vehicle using HSFM

4. Results and Discussions

4.1 Calibration

The calibration of HSFM was carried out for all the filtered trajectories. Since we have filtered the trajectories for small lateral displacements, boundary parameters (s_{0b}^{γ} and f_b) cannot be identified for the vehicles driving at nearly constant lateral distance to the boundary and can be confounded with any other constant effect such as that coming from the desired speed. To overcome this, the value of s_{0b}^{γ} was set to the constant value $s_{0b}^{\gamma} = 0.15$ provided by the literature [18]. To estimate f_b at least globally, we have performed a pool calibration including several trajectories with different lateral positions and boundary values as [0.1,5] m/s². The result f_b =2.4 m/s² which was then used as constant for the individual calibration of trajectories. Figure 5 shows the variation of boundary acceleration with the lateral position of vehicles at this f_b value, computed using Equation (7). The longitudinal deceleration is higher when the vehicle is placed at the boundaries and the values are reduced rapidly towards zero in an exponential manner.

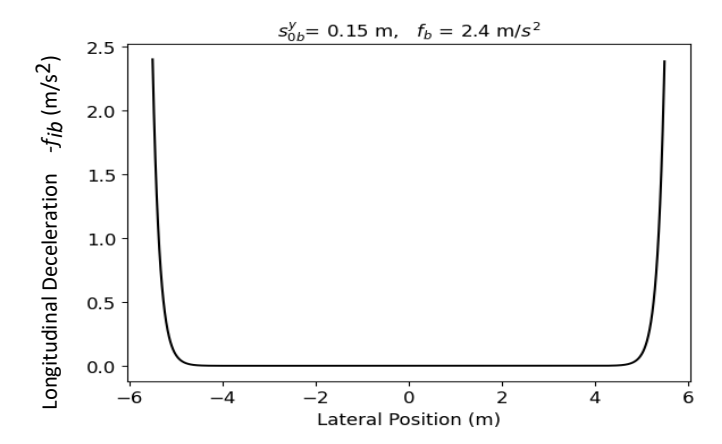


Figure 5 Variation of boundary acceleration with lateral position of the vehicle at optimal f_b value

The frequency distributions of the individually calibrated HSFM parameters are shown in Figure 6 and the summary statistics are provided in Table 1. The average values of parameters are reasonable and comparable with the previous studies [18]. The mean RMSE of the position is found to be 1.05 m, which is reasonable and comparable with the results from a previous study by Chaudhari et al. [13] where the RMSE of the position is reported as 1.692 m. This value is valid for the global approach of calibration, which involves comparing a complete data trajectory with a simulated trajectory. Please refer to Supplemental Material Videos 1 and 2 for an illustration of the calibration capability of the model. The range of most of the desired speed values i.e., 10-20 m/s (Figure 6a), is lower than that observed in homogenous traffic [23] which is expected due to the presence of different types of vehicles and non-lane-based traffic. The average minimum spacing is approximately 1.4 m (Figure 6b) which is lower compared to ordered traffic [21]. This is reasonable and expected since driver characteristics and vehicle types allow the vehicles to maintain lower longitudinal gaps.

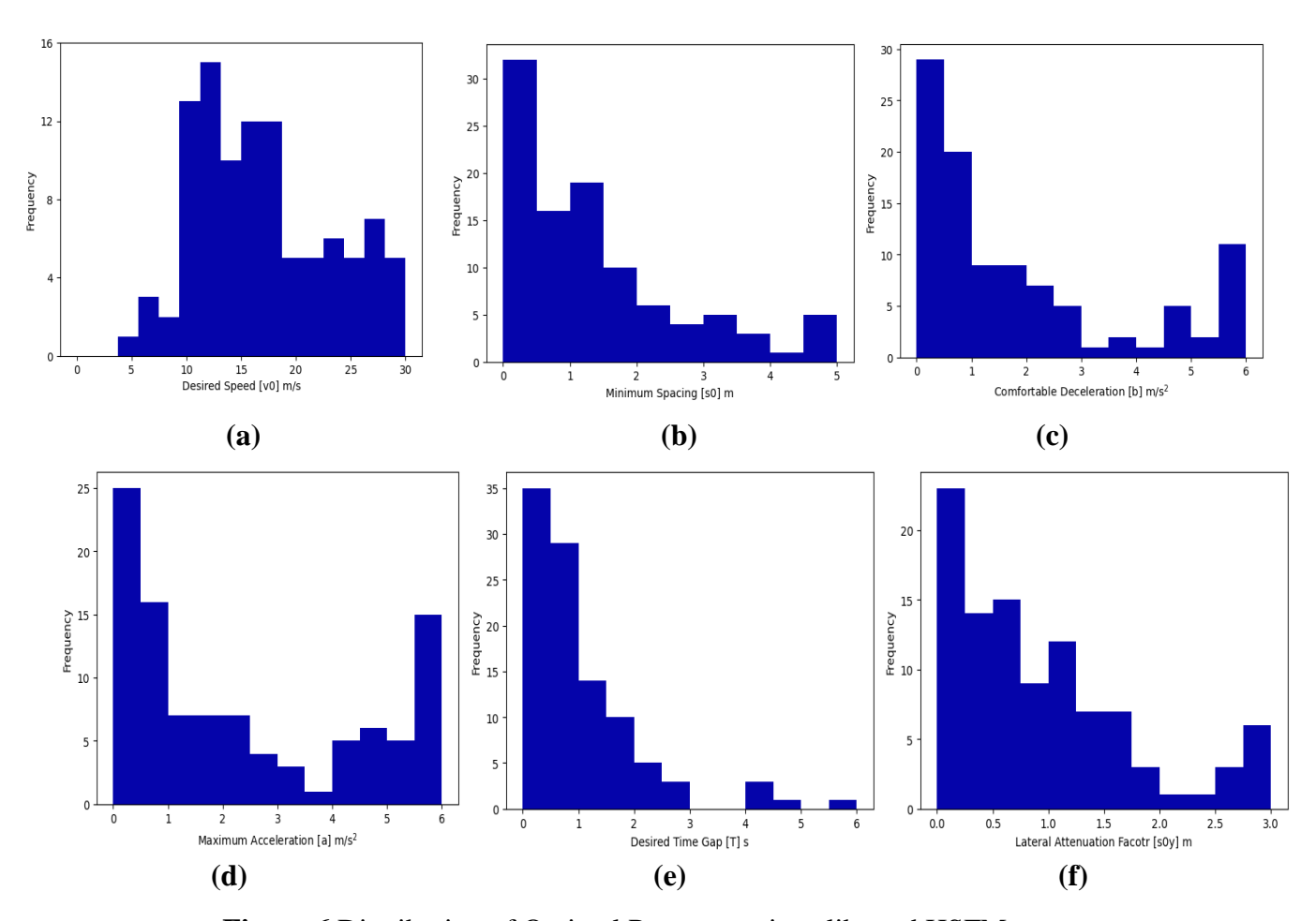


Figure 6 Distribution of Optimal Parameters in calibrated HSFM

Table 1 Descriptive Statistics of Optimal Parameters of HSFM

Model Parameters	Boundary Values	Mean	Median	Standard Deviation	Minimum	Maximum
Desired Speed (v_0) , m/s	[1,30]	16.987	15.891	6.134	4.969	29.761
Desired Spacing (s_0) , m	[0.1,5]	1.405	1.036	1.276	0.107	4.926
Comfortable Deceleration (<i>b</i>), m/s ²	[0.1,6]	1.896	1.076	1.906	0.101	5.987
Maximum Acceleration (a), m/s ²	[0.1,6]	2.399	1.661	2.084	0.115	5.982
Desired Time Gap (T) , s	[0.1,6]	1.055	0.732	1.069	0.104	5.806
Lateral attenuation scale (s_0^y) , m	[0.1,3]	0.944	0.676	0.793	0.105	2.933
RMSE, m	-	1.051	0.748	0.972	0.209	6.858

The desired time gap values being mostly lesser than 1 s (Figure 6e) just reflects a different driving behaviour. A possible reason is that collisions are not considered to be as serious events as in Western countries. The comfortable deceleration and the acceleration values mostly lie below 2 m/s²[14,21]. However, the calibration of some trajectories returns very high acceleration and deceleration values at or near the allowed limit meaning that these parameters cannot be identified for these instances. Most of the values of the lateral attenuation scale (s_{0y}) were found to be less than 1 m (Figure 6f) meaning that such leaders do not exert much repulsive social force, i.e., a lateral gap of 1 m or less is considered as a normal situation.

The distribution for parameters such as desired speed, minimum spacing, and comfortable deceleration for different types of follower vehicles such as TW and Car (Figure 7) are also plotted to assess the difference in parameter distributions and values, and the proportion of other types of following vehicles are small in the data and hence omitted. It is observed that the desired speed of cars is slightly right skewed as it is expected that the cars have desired speeds generally higher than two-wheelers. The distribution of comfortable deceleration and minimum spacing is not significantly different for two-wheelers and cars. To compare and understand the parameter distribution of different types of following vehicles, more data is needed.

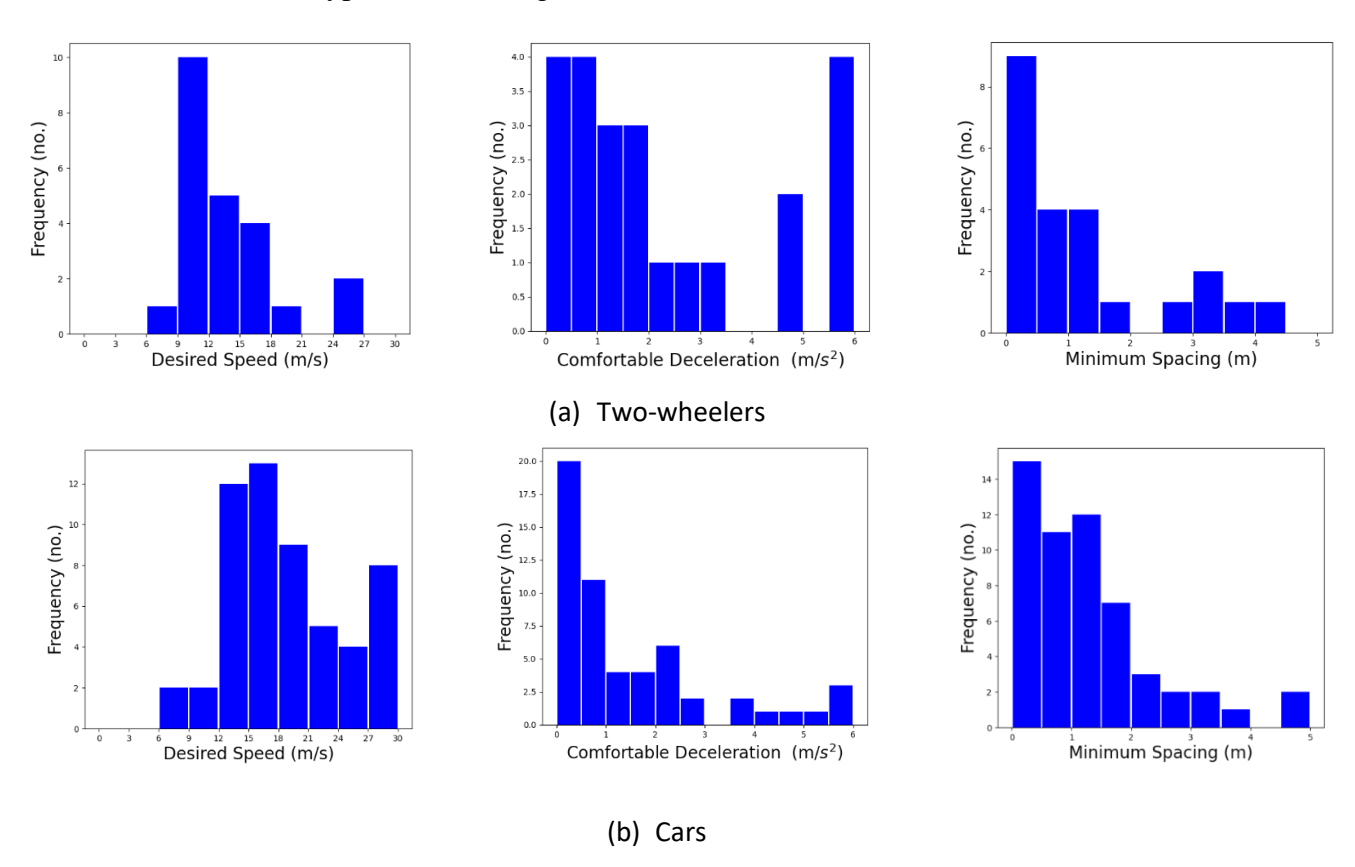


Figure 7 Distribution of Selected Parameters for Two-wheelers and Cars

In general, the following procedure based on kernel smoothing can be used to simulate the heterogeneous traffic using parameter distributions of different types of vehicles including correlations:

- To incorporate appropriate standard deviations and correlation structures into the kernel, a six-dimensional multivariate Gaussian kernel density may be used.
- To determine the kernel, one first determines the components of the sample covariance matrix Σ as follows

$$\Sigma_{jk} = \frac{1}{n-2} \sum_{i=1}^{n} (\beta_{ij} - \overline{\beta_j}) (\beta_{ik} - \overline{\beta_k})$$
 (10)

Where β_{ij} is the parameter estimate β_j as calibrated to the follower trajectory i, and $\overline{\beta_j}$ the mean overall trajectories.

• Depending on the number *d* of the dimensions (parameters) and number *n* of data points (i.e., calibrated trajectories), the so-called bandwidth matrix is chosen as a scaled downed covariance matrix,

$$H = n^{-\frac{2}{d+4}} \Sigma \tag{11}$$

leading to the Gaussian kernel density

$$f_k(\beta) = (2\pi)^{\frac{-d}{2}} |H|^{\frac{1}{2}} e^{\frac{1}{2}\beta^T H^{-1}\beta}$$
(12)

• The estimated density function of the parameter estimates is then given by

$$\hat{f}_{(\beta)} = \frac{1}{n} \sum_{i} f_k (\beta - \beta_i) \tag{13}$$

• Then, use Monte Carlo methods to sample from this distribution in a simulation.

When using these parameter distributions for simulations of heterogeneous traffic including correlations, one needs more data points to approximate the density of the true parameter distribution (generally not Gaussian) using kernel density estimates.

To verify that global minima were found, we checked the results by plotting fitness landscapes around the calibrated parameter values [8]. In Figure 8, contour plots are displayed for some pairs of the parameters of HSFM (desired speed, maximum acceleration, desired time gap, comfortable deceleration, and minimum spacing). In each of the contour plots, the remaining parameters were kept constant at their respective calibrated values. While such fitness landscapes can only check local minima, the large parameter ranges for which the fitness function has been evaluated give evidence that the true global minimum has been found by the GA. Further evidence is provided by observing that the GA results do not depend on the initial guess [8].

In fitness landscapes in Figure 8, it is observed that all the optimal parameter values converged to the global minima and are within the bounded region. In the example shown in Figure 9, however, the value of v_0 is very large and possibly unbounded. This can be explained by observing that the data contain very few points with gaps larger than 40 m which can be attributed to free flow (Figure 8b). Hence, the desired speed is not identified and any value above a certain minimum essentially gives the same dynamics. Notice that this may also apply to other parameters. For example, the acceleration and deceleration parameters are not identified if there are no sufficiently long acceleration or deceleration episodes in the data, the parameters s_0 and T cannot be identified if there is only free traffic, the boundary parameters play no role if a trajectory never approaches a road boundary, and the lateral attenuation parameter cannot be determined if there are no variable

lateral offsets to the leaders. Generally, if certain situations are not included in the data, the corresponding parameters are unobservable and must not be calibrated [8]. Since it is practically difficult to obtain trajectories containing all traffic situations, it is suggested that the missing situations need to be determined before calibration descriptively and the pertaining parameter is set to aspects of the descriptive statistics (e.g., the desired speed to the data maximum), or fixed standard values.

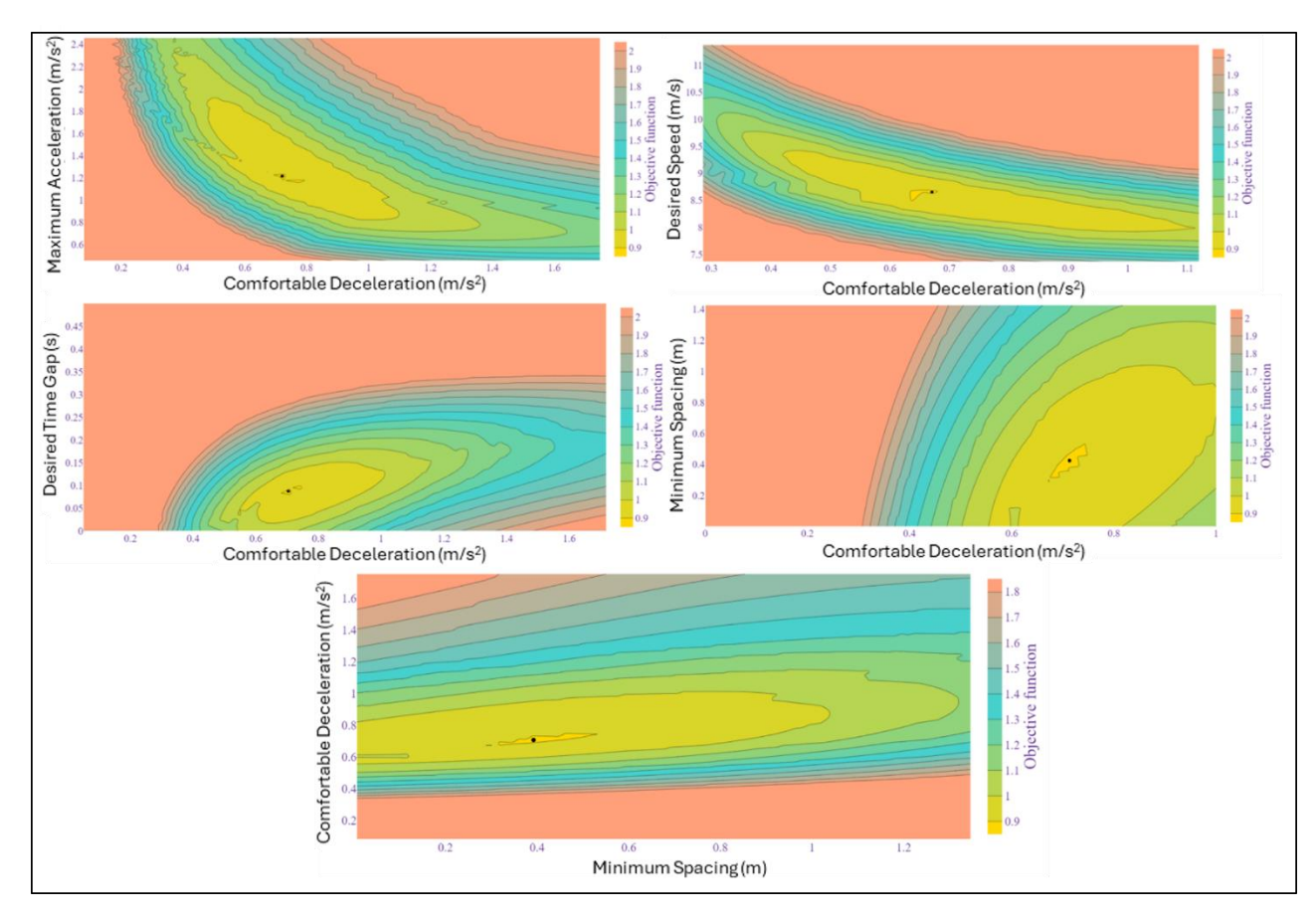


Figure 8 Fitness landscapes for calibrated HSFM parameters with bounded minima (*Note: The black circle in fitness landscape indicates the optimal parameters*)

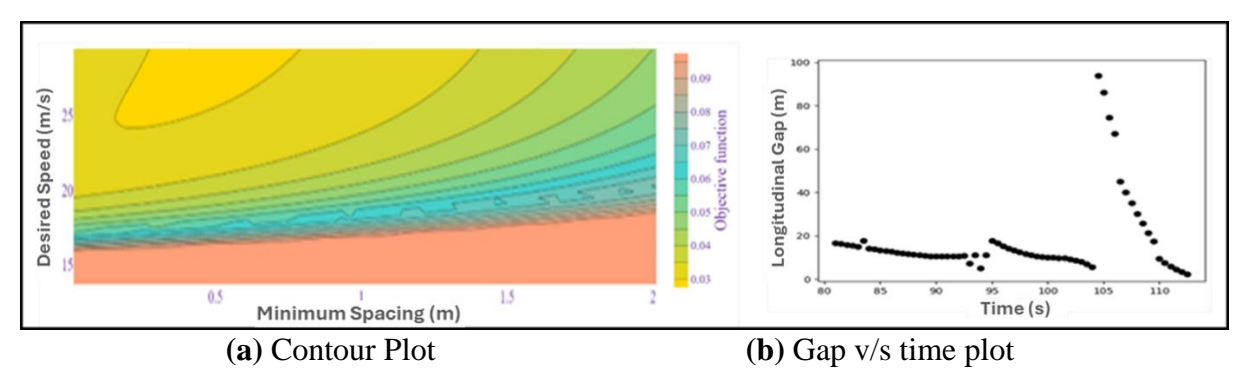


Figure 9 Fitness landscapes for calibrated HSFM parameters with unbounded minimum

Finally, we emphasize that the proposed calibration protocol allows for several leaders during the trajectory time interval which is often observed frequently. Figure 10 displays, in addition to the calibration result, the longitudinal and lateral gap between the subject vehicle and the instantaneous most influencing leader for two, three, and four leaders (Figures 10a, 10b, and 10c, respectively). In Figure 10a, the most influential leader changes at t=446 s and in Figure 10b there are three different most influencing leaders for the time intervals 287 s to 310 s, 310 s to 316 s, and 316 s to 325 s, respectively. From the plots, it is understood that the calibrated HSFM performs well in the prediction of longitudinal dynamics irrespective of the following or non-following behavior.

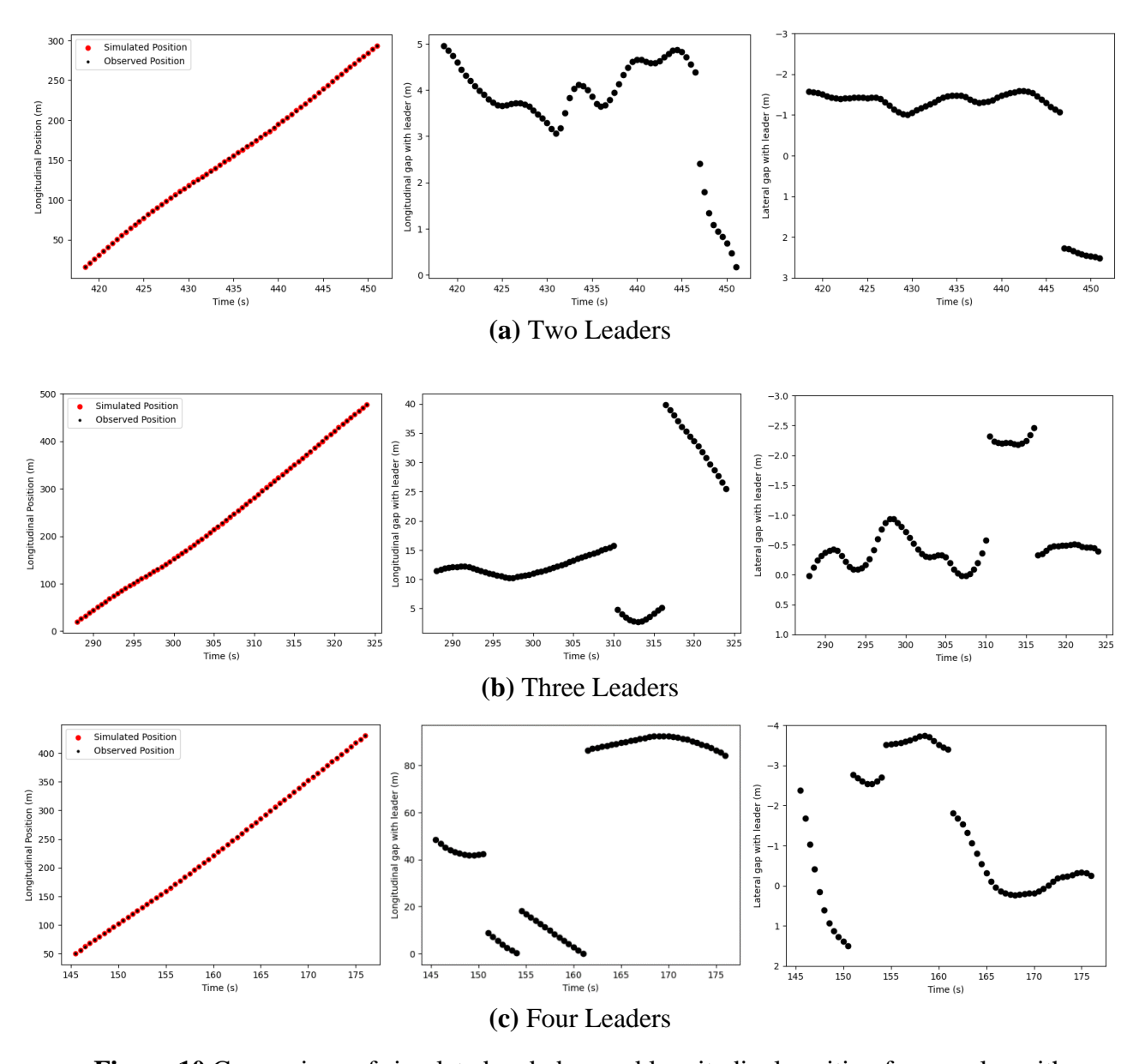


Figure 10 Comparison of simulated and observed longitudinal position for samples with different leaders throughout the movement

5. Conclusions

The present study aims to calibrate the High-speed Social-Force model (HSFM) to model the longitudinal dynamics of vehicles under disordered traffic conditions. The trajectory data used for the calibration purpose has been collected at a road section in Chennai city with a study stretch of length 610 m which is significantly longer than that of past studies of disordered traffic and allows, for the first time, a calibration of the behavior of individual followers including the parameters for the response to a lateral displacement, i.e., leader identification and the transition from following to non-following behavior.

This study is mainly focused on the longitudinal dynamics of vehicles and therefore, it was ensured that only vehicle trajectories without significant lateral movements were considered for calibration. The longitudinal position of the vehicle was used as the measure of performance and the RMS error was minimized using a genetic algorithm to obtain the calibrated HSFM parameters. The calibration errors are within the acceptable range. The parameters were also verified for the attainment of the global minima by plotting the fitness landscapes. It was found that the parameters attained the global optima successfully. However, if certain situations are not included in the data due to incompleteness, the corresponding parameters are unobservable and must not be calibrated.

The vehicle-type-based calibration was not considered due to the constraints in the quantity of the data. To address this, in a recent study by the authors [26], a long trajectory dataset of 560 m road length has been created by UAV cameras with a higher time resolution of 0.04 s. Moreover, vehicle detection is carried out using a fully automated tool developed using deep learning algorithms. The future scope of the study is to integrate the calibrated longitudinal dynamics model with lateral movement models that would be incorporated into the simulation models for realistic outcomes.

Acknowledgments

The authors acknowledge the support for this study as a part of the Scheme for Promotion of Academic and Research Collaboration (SPARC) project funded by the Ministry of Education, Government of India (Project No. SPARC/2019-2020/P2384/SL). The authors would also like to acknowledge the support provided by the Science and Engineering Research Board, Department of Science and Technology under the Visiting Advanced Joint Research Faculty Scheme (VJR/2021/000016).

References

- [1] Asaithambi, G., Kanagaraj, V., & Toledo, T. (2016). Driving behaviors: Models and challenges for non-lane based mixed traffic. *Transportation in Developing Economies*, 2, 1-16.
- [2] Li, Y., Zhang, L., Peeta, S., Pan, H., Zheng, T., Li, Y., & He, X. (2015). Non-lane-discipline-based car-following model considering the effects of two-sided lateral gaps. *Nonlinear Dynamics*, 80, 227-238.
- [3] Gunay, B. (2009, February). Rationality of a non-lane-based car-following theory. In *Proceedings of the Institution of Civil Engineers-Transport* (Vol. 162, No. 1, pp. 27-37). Thomas Telford Ltd.

- [4] Budhkar, A. K., & Maurya, A. K. (2017). Characteristics of lateral vehicular interactions in heterogeneous traffic with weak lane discipline. *Journal of Modern Transportation*, 25, 74-89.
- [5] Azam, M. S., Bhaskar, A., & Haque, M. M. (2022). Driving behaviour modelling in the context of heterogeneous traffic and poor lane discipline conditions: state of the art and beyond. *Transportmetrica A: transport science*, 18(3), 367-434.
- [6] Treiber, M., & Kesting, A. (2013). Traffic flow dynamics. *Traffic Flow Dynamics: Data, Models and Simulation, Springer-Verlag Berlin Heidelberg*, 983-1000.
- [7] Brockfeld, E., Kühne, R. D., & Wagner, P. (2004). Calibration and validation of microscopic traffic flow models. *Transportation Research Record*, 1876(1), 62-70.
- [8] Treiber, M., & Kesting, A. (2013). Microscopic calibration and validation of car-following models—a systematic approach. *Procedia-Social and Behavioral Sciences*, 80, 922-939.
- [9] Anand, P. A., Atmakuri, P., Anne, V. S. R., Asaithambi, G., Srinivasan, K. K., Sivanandan, R., & Chilukuri, B. R. (2019). Calibration of vehicle-following model parameters using mixed traffic trajectory data. *Transportation in Developing Economies*, 5, 1-11.
- [10] Maheshwary, P., Bhattacharyya, K., Maitra, B., & Boltze, M. (2017). A methodology for calibration of vehicle class-wise driving behavior in heterogeneous traffic environment. In *World Conf Transp Res* 00 (pp. 1-15).
- [11] Raju, N., Arkatkar, S., & Joshi, G. (2020). Evaluating performance of selected vehicle following models using trajectory data under mixed traffic conditions. *Journal of Intelligent Transportation Systems*, 24(6), 617-634.
- [12] Raju, N., Arkatkar, S., & Joshi, G. (2021). Modeling following behavior of vehicles using trajectory data under mixed traffic conditions: an Indian viewpoint. *Transportation Letters*, *13*(9), 649-663.
- [13] Anil Chaudhari, A., Srinivasan, K. K., Rama Chilukuri, B., Treiber, M., & Okhrin, O. (2022). Calibrating Wiedemann-99 model parameters to trajectory data of mixed vehicular traffic. *Transportation Research Record*, 2676(1), 718-735.
- [14] Zhu, M., Wang, X., & Tarko, A. (2018). Modeling car-following behavior on urban expressways in Shanghai: A naturalistic driving study. *Transportation research part C:* emerging technologies, 93, 425-445.
- [15] Kashyap NR, M., Sivagnanasundaram, K., Kanagaraj, V., Asaithambi, G., & Toledo, T. (2022). Investigation of car-following models in disordered traffic using trajectory data obtained from unmanned aerial vehicles. *Transportation Letters*, 1-11.
- [16] Asaithambi, G., Kanagaraj, V., Srinivasan, K. K., & Sivanandan, R. (2018). Study of traffic flow characteristics using different vehicle-following models under mixed traffic conditions. *Transportation Letters*, 10(2), 92-103.
- [17] Raju, N., Arkatkar, S., Easa, S., & Joshi, G. (2022). Customizing the following behavior models to mimic the weak lane based mixed traffic conditions. *Transportmetrica B: transport dynamics*, 10(1), 20-47.
- [18] Kanagaraj, V., & Treiber, M. (2018). Self-driven particle model for mixed traffic and other disordered flows. *Physica A: Statistical Mechanics and its Applications*, 509, 1-11.
- [19] Treiber M. & Anil Chaudhari A. (2022) The intelligent agent model a fully two-dimensional microscopic traffic flow model. *Traffic and Granular Flow, IIT Delhi*.

- [20] Karimi, M., & Alecsandru, C. (2019). Two-fold calibration approach for microscopic traffic simulation models. *IET Intelligent Transport Systems*, 13(10), 1507-1517.
- [21] Kurtc, V. (2020). Studying car-following dynamics on the basis of the HighD dataset. *Transportation Research Record*, 2674(8), 813-822.
- [22] Punzo, V., & Montanino, M. (2016). Speed or spacing? Cumulative variables, and convolution of model errors and time in traffic flow models validation and calibration. *Transportation Research Part B: Methodological*, 91, 21-33.
- [23] Kesting, A., & Treiber, M. (2008). Calibrating car-following models by using trajectory data: Methodological study. *Transportation Research Record*, 2088(1), 148-156.
- [24] Saifuzzaman, M., Zheng, Z., Haque, M. M., & Washington, S. (2015). Revisiting the Task—Capability Interface model for incorporating human factors into car-following models. *Transportation Research Part B: Methodological*, 82, 1-19.
- [25] Sharma, A., Zheng, Z., & Bhaskar, A. (2019). Is more always better? The impact of vehicular trajectory completeness on car-following model calibration and validation. *Transportation Research Part B: Methodological*, 120, 49-75.
- [26] Rajput, S., Shivachethan, V., Kanagaraj, V., Asaithambi, G. and Treiber, M. Obtaining long trajectory data of disordered traffic using a swarm of unmanned aerial vehicles. (Unpublished)